The Journal of Chemical Physics

RESEARCH ARTICLE | MAY 20 2022

Finite-temperature atomic relaxations: Effect on the temperature-dependent C_{44} elastic constants of Si and BAs

Cristiano Malica ✉ ; Andrea Dal Corso

J. Chem. Phys. 156, 194111 (2022)
https://doi.org/10.1063/5.0093376

The Journal of Chemical Physics ARTICLE scitation.org/journal/jcp

Finite-temperature atomic relaxations: Effect on the temperature-dependent C_{44} elastic constants of Si and BAs

Cite as: J. Chem. Phys. 156, 194111 (2022); doi: 10.1063/5.0093376
Submitted: 28 March 2022 • Accepted: 3 May 2022 •
Published Online: 20 May 2022

Cristiano Malica[1,a] and Andrea Dal Corso[1,2]

AFFILIATIONS

[1] International School for Advanced Studies (SISSA), Via Bonomea 265, 34136 Trieste, Italy
[2] IOM-CNR, 34136 Trieste, Italy

[a] Author to whom correspondence should be addressed: malicacristiano@gmail.com

ABSTRACT

The effect of atomic relaxations on the temperature-dependent elastic constants (TDECs) is usually taken into account at zero temperature by the minimization of the total energy at each strain. In this paper, we investigate the order of magnitude of this approximation on a paradigmatic example: the C_{44} elastic constant of diamond and zincblende materials. We estimate the effect of finite-temperature atomic relaxations within the quasi-harmonic approximation by computing *ab initio* the internal strain tensor from the second derivatives of the Helmholtz free-energy with respect to strain and atomic displacements. We apply our approach to Si and BAs and find a visible difference between the softening of the TDECs computed with the zero-temperature and finite-temperature atomic relaxations. In Si, the softening of C_{44} passes from 8.6% to 4.5%, between T = 0 K and T = 1200 K. In BAs, it passes from 8% to 7%, in the same range of temperatures. Finally, from the computed elastic constant corrections, we derive the temperature-dependent Kleinman parameter, which is usually measured in experiments.

I. INTRODUCTION

Elastic constants are important quantities for crystal thermodynamics and have a wide field of applications. For example, they determine crystal stability, thermal expansion, and thermal stresses. In particular, temperature-dependent elastic constants (TDECs) allow prediction of seismic properties of materials, basic information to probe the interior of planets in geophysics.[1]

With the increase in power and number of central processing units of modern high performance computers, *ab initio* calculation of TDECs and other thermal properties is becoming more and more affordable for a large class of materials, both isotropic and anisotropic (with one or more lattice parameters).

Several authors have calculated the TDECs and thermodynamic properties of solids, but there is still a need to compare different methods and approximations among themselves in order to choose the best ones for routine calculations. In a previous work,[2] we compared the two main methods used for calculation of the TDECs: the quasi-static approximation (QSA) and the quasi-harmonic approximation (QHA). The QSA accounts only for the thermal expansion of the solid by computing the ECs from the second derivatives of the energy with respect to the strain at different volumes (or crystal parameters). The QHA provides the TDECs from the second derivatives of the Helmholtz free-energy with respect to the strain. In our examples, the QHA, although computationally more demanding, gave results closer to the experiment than the QSA.

We have also investigated the effect of electronic excitation in the TDECs of simple metals. We showed that this effect is relevant for the temperature dependence of the C_{44} ECs of Pd and Pt with partially filled *d*-shells, while in Cu and Au, having completely filled *d*-shells, the effect is negligible.[3]

One further approximation for the calculation of the TDECs consists of determining the internal atomic relaxations at zero temperature (i.e., by minimizing the total energy with respect to the

atomic displacements) and using them at all temperatures. This approximation is often referred to as the zero static internal stress approximation (ZSISA).[4]

Indeed, in order to compute the ECs, we need to use several strains to deform the unit cell. These strains could change the distances between atoms, and if not in high symmetry positions, the atoms might relax in a different configuration. In this case, the *frozen-ion* (FI) ECs calculated with the uniformly strained atomic positions might differ from the *relaxed-ion* (RI) ECs where the atoms are allowed to relax. At $T = 0$ K, there are two methods to compute the RI ECs: (i) the direct relaxation of atoms by imposing vanishing forces on them (i.e., minimizing the total energy with respect atomic displacements) or (ii) the calculation of the FI ECs and the addition of the correction due to internal strain (computed as the second derivatives of the total energy with respect to the displacements and strains). At $T = 0$ K, the two methods give identical results.

In the calculations of the TDECs within the QHA, the atoms are usually relaxed at $T = 0$ K by using the ZSISA. The ZSISA is consistent with the QSA, which deals with the derivatives of the energy, but it is not within the QHA for which a proper minimization of the free-energy with respect to the atomic displacements should be carried out. An attempt to compute the finite-temperature atomic relaxations beyond the ZSISA was made, within a shell model, in Refs. 5 and 6 by estimating analytically the derivatives of the free-energy with respect to internal displacements.

In this work, after the comparison of the two methods to compute the RI ECs at zero temperature, we will generalize the internal strain approach at finite temperature by computing the mixed second derivatives of the Helmholtz free-energy with respect to atomic displacements and strains in a set of geometries and interpolating at each temperature in such a way to obtain the correction to the FI ECs at the minimum of the free-energy.

The direct relaxation and internal strain methods are compared at $T = 0$ K for Si, C, SiC, GaAs, and BAs, showing a very good agreement in each case. Then, we apply the finite-temperature internal strain formalism for the TDECs of Si and BAs that were previously calculated within the ZSISA.[2,7] In these materials, internal relaxations affect only the C_{44} EC, and we found visible differences in the temperature dependence, especially in Si. The temperature induced softening passes from 8.6% (within the ZSISA) to 4.5% (within the temperature-dependent atomic relaxation) in the range of 0–1200 K for Si and from 8% (within the ZSISA) to 7% (with the temperature-dependent atomic relaxation) in the same range of temperatures for BAs. Hence, the internal strain calculated from the derivatives of the free-energy leads to a smaller softening of the C_{44} ECs. The internal strain of diamond and zincblende materials is often measured experimentally in terms of the so-called Kleinman parameter. We deduce the temperature dependence of this parameter from the correction to the C_{44} EC.

II. THEORY

The total energy can be written as a function of both the atomic displacements $u_{s\alpha}$ and strain $\epsilon_{\alpha\beta}$. If we consider a solid with vanishing atomic forces and stresses, its Taylor expansion in atomic units (a.u.) up to the second order is

$$E(\{u_{s\alpha}\},\{\epsilon_{\alpha\beta}\}) = E_0 + \frac{1}{2}\sum_{s\alpha s'\beta}\Phi_{s\alpha s'\beta}u_{s\alpha}u_{s'\beta} + \frac{\Omega}{2}\sum_{\alpha\beta\gamma\delta}C^{FI}_{\alpha\beta\gamma\delta}\epsilon_{\alpha\beta}\epsilon_{\gamma\delta} - \sum_{s\alpha\beta\gamma}\Lambda_{s\alpha\beta\gamma}u_{s\alpha}\epsilon_{\beta\gamma}. \quad (1)$$

The term quadratic in the displacements defines the interatomic force constant tensor as follows:

$$\Phi_{s\alpha s'\beta} = \frac{\partial^2 E}{\partial u_{s\alpha}\partial u_{s'\beta}}, \quad (2)$$

which is related to the dynamical matrix $\frac{\Phi_{s\alpha s'\beta}}{\sqrt{M_s M_{s'}}}$ at the reciprocal lattice point $\mathbf{q} = 0$. The term quadratic in the strain defines the *FI* elastic constant tensor as follows:

$$C^{FI}_{\alpha\beta\gamma\delta} = \frac{1}{\Omega}\frac{\partial^2 E}{\partial\epsilon_{\alpha\beta}\partial\epsilon_{\gamma\delta}}, \quad (3)$$

where Ω is the volume of the unit cell. The mixed second derivative with respect to the displacement and strain defines the following tensor:

$$\Lambda_{s\alpha\beta\gamma} = -\frac{\partial^2 E}{\partial u_{s\alpha}\partial\epsilon_{\beta\gamma}}, \quad (4)$$

whose components are the so-called internal strain parameters. If $\Lambda_{s\alpha\beta\gamma}$ is non-zero, the equilibrium displacement of atom s in the direction α is proportional to the strain as follows:

$$u_{s\alpha} = \sum_{s'\beta\gamma\delta}\Phi^{-1}_{s\alpha s'\beta}\Lambda_{s'\beta\gamma\delta}\epsilon_{\gamma\delta}, \quad (5)$$

where $\Phi^{-1}_{s\alpha s'\beta}$ is the inverse of (2) and can be written as follows:

$$\Phi^{-1}_{s\alpha s'\beta} = \sum_{\nu}\frac{e^{\nu}_{s\alpha}e^{\nu}_{s'\beta}}{\sqrt{M_s M_{s'}}\omega^2_{\nu}}, \quad (6)$$

where M_s and $M_{s'}$ are the masses of atoms s and s', respectively. The sum (related to $\mathbf{q} = 0$) is over all optical modes ν;[8] $e^{\nu}_{s\alpha}$ and $e^{\nu}_{s'\beta}$ are the α and β components of the eigenvectors of mode ν of atoms s and s', respectively; and ω^2_{ν} are the eigenvalues for the mode ν. They satisfy the eigenvalue equation

$$\sum_{s'\beta}\frac{1}{\sqrt{M_s M_{s'}}}\Phi_{s\alpha s'\beta}e^{\nu}_{s'\beta} = \omega^2_{\nu}e^{\nu}_{s\alpha}. \quad (7)$$

If we substitute the displacement (5) $u_{s\alpha}$ into expansion (1) $E(\{u_{s\alpha}\},\{\epsilon_{\alpha\beta}\})$ and consider the terms quadratic in the strain, we obtain

$$E = E_0 + \frac{\Omega}{2}\sum_{\lambda\mu\gamma\delta}C_{\lambda\mu\gamma\delta}\epsilon_{\lambda\mu}\epsilon_{\gamma\delta}, \quad (8)$$

where $C_{\lambda\mu\gamma\delta}$ is the EC tensor with the correction due to the internal strain (RI ECs) and is equal to

$$C_{\lambda\mu\gamma\delta} = C^{FI}_{\lambda\mu\gamma\delta} - \Delta C_{\lambda\mu\gamma\delta}, \tag{9}$$

where

$$\Delta C_{\lambda\mu\gamma\delta} = \frac{1}{\Omega}\sum_{s\alpha}\Lambda_{s\alpha\lambda\mu}\Gamma_{s\alpha\gamma\delta} \tag{10}$$

and

$$\Gamma_{s\alpha\gamma\delta} = \sum_{s'\beta}\Phi^{-1}_{s\alpha s'\beta}\Lambda_{s'\beta\gamma\delta}. \tag{11}$$

Now, we consider the zincblende structure with two different atoms with masses M_1 and M_2 (the diamond case will be obtained for $M_1 = M_2$). For this crystal, the following symmetry relation is valid for the internal strain tensor:[9]

$$\Lambda_{1\beta\gamma\delta} = -\Lambda_{2\beta\gamma\delta} = \Lambda|\epsilon_{\beta\gamma\delta}|, \tag{12}$$

for which the internal strain of atom 1 is equal and opposite to the one of atom 2, Λ is a constant, and $\epsilon_{\beta\gamma\delta}$ is the Levi-Cività tensor that is 1 when all its indices are different and 0 otherwise. Expanding the sum (11) over the two atoms and using the previous symmetry relation, we have

$$\Gamma_{s\alpha\gamma\delta} = \sum_{\nu\beta}\frac{e^{\nu}_{s\alpha}}{\sqrt{M_s}\omega^2_{\nu}}\Lambda|\epsilon_{\beta\gamma\delta}|\left(\frac{e^{\nu}_{1\beta}}{\sqrt{M_1}} - \frac{e^{\nu}_{2\beta}}{\sqrt{M_2}}\right). \tag{13}$$

In the previous sum over the modes ν, only the optical modes at Γ contribute because within the acoustic modes, the two atoms move in phase and have equal displacements ($\frac{e^{\nu}_{1\beta}}{\sqrt{M_1}} = \frac{e^{\nu}_{2\beta}}{\sqrt{M_2}}$), and hence, the term in parenthesis in Eq. (13) vanishes. Now, we substitute in Eq. (13) the expression of the eigenvectors of the optical modes,

$$e^{\nu}_{s\alpha} = \frac{1}{\sqrt{3}\sqrt{M_1+M_2}}\begin{pmatrix}\sqrt{M_2}\\ \sqrt{M_2}\\ \sqrt{M_2}\\ -\sqrt{M_1}\\ -\sqrt{M_1}\\ -\sqrt{M_1}\end{pmatrix}. \tag{14}$$

The displacement corresponding to this eigenvector is discussed in the Appendix. Rearranging the terms and introducing the reduced mass μ, we have

$$\Gamma_{s\alpha\delta\epsilon} = \sum_{\nu\beta}\frac{e^{\nu}_{s\alpha}}{\sqrt{M_s}\omega^2_{\nu}}\frac{1}{\sqrt{3}}\Lambda|\epsilon_{\beta\gamma\delta}|\frac{1}{\sqrt{\mu}}. \tag{15}$$

Now, we insert $\Gamma_{s\alpha\delta\epsilon}$ in Eq. (10) and use Eq. (12) again and the components of optical eigenvectors (14). We have

$$\Delta C_{\lambda\mu\gamma\delta} = \frac{1}{3\Omega}\sum_{\alpha\beta\nu}\frac{\Lambda^2}{\mu\omega^2_{\nu}}|\epsilon_{\beta\gamma\delta}||\epsilon_{\alpha\lambda\mu}|. \tag{16}$$

The only non-zero correction is $\Delta C_{44} = \Delta C_{2323}$ (the correction is the same for C_{55} and C_{66} that are equal to C_{44} in cubic solids[2]). In this case, the sum of α and β of the module of the Levi-Cività tensor leads to unitary multiplicative factors, while the sum over the optical modes remains. The result is

$$\Delta C_{44} = \frac{1}{3\Omega}\frac{\Lambda^2}{\mu}\sum_{\nu}\frac{1}{\omega^2_{\nu}} = \frac{\Lambda^2}{\Omega\,\mu\,\omega^2_{TO}}. \tag{17}$$

The previous equation gives the correction to the frozen-ion C_{44} elastic constant due to the atomic relaxation and is exact for diamond structures where the longitudinal and transverse optical frequencies are equal $\omega_{LO} = \omega_{TO}$. The proper treatment for polar materials (as BAs) with $\omega_{LO} \neq \omega_{TO}$ requires the introduction of the electric field terms in the free-energy expansion. However, we expect small contributions due to the electric field, and hence, we use Eq. (17) also for polar materials as in Ref. 10.

In the literature, the correction (17) is often written in terms of the so-called Kleinman parameter ξ[10] as follows:

$$\Delta C_{44} = \frac{\mu\,\omega^2_{TO}}{4\,a_0}\xi^2, \tag{18}$$

where a_0 is the lattice constant of the cubic crystal. If we apply a rhombohedral strain $\epsilon_F = \frac{1}{2}\epsilon_4(1-\delta_{ij})^2$ to the zincblende crystal, the actual elongation of the [111] bond is $(1-\xi)\epsilon_4 a\sqrt{3}/4$ so that $\xi = 0$ corresponds to a uniform strain of the atomic positions, while $\xi = 1$ means that the bond remains rigid. By comparing Eq. (17) with Eq. (18), we obtain the Kleinman parameter in terms of the internal strain parameter as follows:

$$\xi = \frac{\Lambda}{\mu\,\omega^2_{TO}\frac{a_0}{4}}. \tag{19}$$

In Secs. III and IV, we present our calculations of ΔC_{44} and ξ from Eqs. (17) and (19) by using the internal-strain formulation at $T = 0$ K for some materials with diamond and zincblende structures: Si, C, SiC, GaAs, and BAs. Then, we compare with ΔC_{44} calculated from direct atomic relaxation. Finally, we estimate the same correction at finite temperature for the TDECs C_{44} of Si and BAs using the Helmholtz free-energy instead of the energy in the grid of strains and displacements,

$$\Lambda_{s\alpha\beta\gamma} = -\frac{\partial^2 F}{\partial u_{s\alpha}\partial\epsilon_{\beta\gamma}}. \tag{20}$$

The Helmholtz free-energy F has the form derived from the QHA[2] and requires the calculation of the phonon dispersions in the strain-displacement grid. The other parameter entering in Eq. (19) ω_{TO} is obtained by interpolating the volume-dependent frequency at the temperature-dependent volume.

III. METHOD

The calculations presented in this work were carried out using density functional theory (DFT) as implemented in the Quantum ESPRESSO package.[12,13] For the calculation of TDECs (FI and RI at $T = 0$ K), we use the thermo_pw code[14] with the formulation presented in Refs. 2, 3, 15, and 16.

For the calculation of the internal strain Λ at $T = 0$ K [Eq. (4)], the total energy is computed in a two-dimensional grid of displacements and strains and fitted with a second degree polynomial. The second derivative of the polynomial is evaluated analytically. The grid for the entries of the rhombohedral strain ϵ_F[2,15] was $(-0.01, -0.005, 0, 0.005, 0.01)$ for all materials. We used a rhombohedral cell having the atomic bond along the z direction. The first atom is fixed in the origin, and the displacements are set moving the second atom in an uniform grid of five positions with distance $\Delta u = 0.05$ a.u. centered at the equilibrium bond-length of the two atoms in the unstrained cubic cell $\frac{\sqrt{3}}{4}a_0$, where a_0 is the equilibrium lattice constant listed in Table I. Then, the atomic displacements are obtained by subtracting these uniform atomic positions from the uniformly strained atomic positions for each strain. We change simultaneously all the six components of the strain ϵ_F and all the three components of the second atom position (the atomic displacement along the z direction in the rhombohedral cell corresponds to a movement in the [111] direction in the cubic cell involving an equal change of all three atomic position components) and compute the derivative of the total energy with respect to these changes, obtaining the quantity Λ', different from the derivative (4), which is, instead, computed with respect to the change of a single component.[17] This translates in a multiplicative factor such that $\Lambda = \frac{\sqrt{3}}{6}\Lambda' = \frac{1}{2\sqrt{3}}\Lambda'$. Hence, this correction allows us to use the rhombohedral cell for each strained configuration and change simply the position of the second atom in the z direction.

The exchange and correlation functional is approximated by the local-density approximation (LDA)[18] for all materials. The pseudopotentials[19] used for each atomic species are reported in the note.[20] For all materials, the cutoff for the wave functions (charge density) was 90 Ry (1300 Ry) and the **k**-point mesh was $16 \times 16 \times 16$.

The finite-temperature correction was applied to Si and BAs for which the contribution of the vibrational free-energy is added in the calculation of Λ. Phonon dispersions are computed in the same two-dimensional grid of strains and displacements defined before. For both materials, DFPT[21,22] was used to calculate the dynamical matrices on a $4 \times 4 \times 4$ **q**-point grid. The dynamical matrices have been Fourier interpolated on a $200 \times 200 \times 200$ **q**-point mesh to evaluate the free-energy. The grids of reference geometries for the TDEC calculation were centered at the $T = 0$ K lattice constant reported in Table I and set in the same way as done for the QHA TDECs[2,7] (nine reference geometries with lattice constants separated from each other by $\Delta a = 0.05$ a.u.). The finite-temperature internal-strain calculation is done for all the reference configurations. A second degree polynomial has been used to fit the Helmholtz free-energy as a function of the strain and displacements to determine Λ at each geometry and temperature. Λ is used to obtain the correction ΔC_{44} [Eq. (17)] for the frozen-ion TDECs at each reference geometry. For the calculation of ΔC_{44}, we used ω_{TO} corresponding to the considered volume $\{\Omega_i\}$. Then, a fourth degree polynomial was used to interpolate $C_{44}(T, \Omega_i)$ at $\Omega(T)$.

TABLE I. Correction to the C_{44} EC: ΔC_{44}^{rel} is computed via direct atomic relaxation, and ΔC_{44}^{IS} and ξ are computed by using the internal-strain formalism. ξ is also compared with other sources when available. C_{44}^{FI} is the frozen-ion EC. The lattice constant a_0 is in a.u., the phonon angular frequency ω_{TO} is in cm^{-1}, C_{44}^{FI} and ΔC_{44} are in kbar, ξ is dimensionless, and Λ is in Ry/a.u. The atomic positions in the diamond and zincblende crystals are (0,0,0) and $\left(\frac{1}{4}, \frac{1}{4}, \frac{1}{4}\right)$ in units of a_0.

	a_0	ω_{TO}	C_{44}^{FI}	ΔC_{44}^{rel}	ΔC_{44}^{IS}	ξ	Λ
Si	10.2065	513	1060	299	299	0.54, 0.53[a], 0.74[a]	0.389
C	6.6821	1320	5971	72	74	0.13	0.173
SiC	8.1835	798	2840	313	320	0.42, 0.38[b], 0.49[c]	0.347
GaAs	10.6085	269	799	218	209	0.55, 0.48[a]	0.290
BAs	8.9660	704	1772	212	213	0.38	0.304

[a]Reference 10.
[b]Reference 9.
[c]Reference 11.

IV. APPLICATIONS

In Table I, we report the equilibrium lattice constants a_0 of Si, C, SiC, GaAs, and BAs. The calculation of the correction ΔC_{44}^{rel} computed from direct atomic relaxation is in good agreement with the one computed with the internal-strain formalism: the largest difference is 9 kbar, found for GaAs. In addition, our Kleinman parameters are in reasonable agreement with those found in the literature. For Si, we have $\xi = 0.54$, in good agreement with the calculation of Ref. 10 ($\xi = 0.53$). For slightly larger differences in GaAs, we have $\xi = 0.55$, while Ref. 10 reported $\xi = 0.48(2)$. Our estimate for SiC is $\xi = 0.42$ and is in between the results of Ref. 9 ($\xi = 0.38$) and Ref. 11 ($\xi = 0.49$). Hence, Eq. (17) gives a quite good estimate in the case of polar materials as well.

Now, we pass to describe the results obtained from the internal strain formalism at finite temperatures. Previous results about the thermal expansion and the TDECs within the ZSISA of Si can be found in Refs. 2 and 24. In Fig. 1, we compare the C_{44} EC of Si as a function of temperature computed with FI (blue line), with

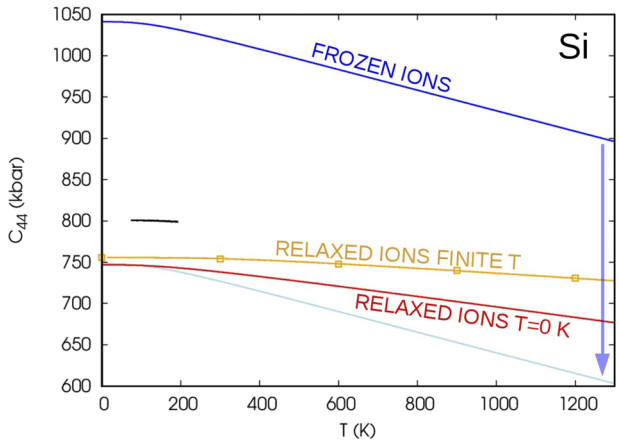

FIG. 1. Temperature-dependent C_{44} elastic constant of Si within the QHA computed with frozen-ions (blue), relaxed-ions at $T = 0$ K (red), and relaxed-ions at finite T (yellow). The frozen-ion result is translated below (light-blue curve) to compare the temperature dependence with the relaxed-ion results. Experimental data are taken from the study by McSkimin[23] (black line).

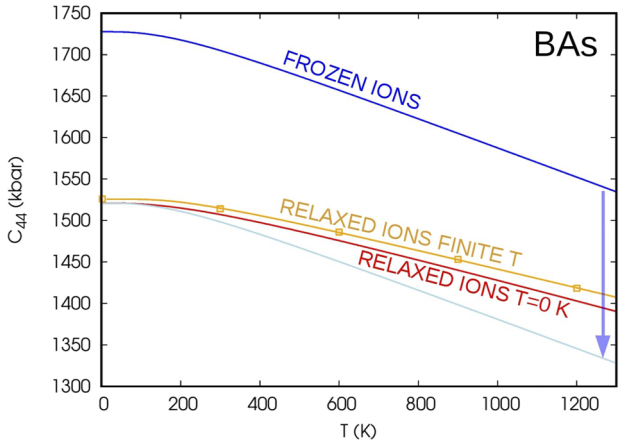

FIG. 2. Temperature-dependent C_{44} elastic constant of BAs within the QHA computed with frozen-ions (blue), relaxed-ions at $T = 0$ K (red), and relaxed-ions at finite T (yellow). The frozen-ion result is translated below (light-blue curve) to compare the temperature dependence with the relaxed-ion results.

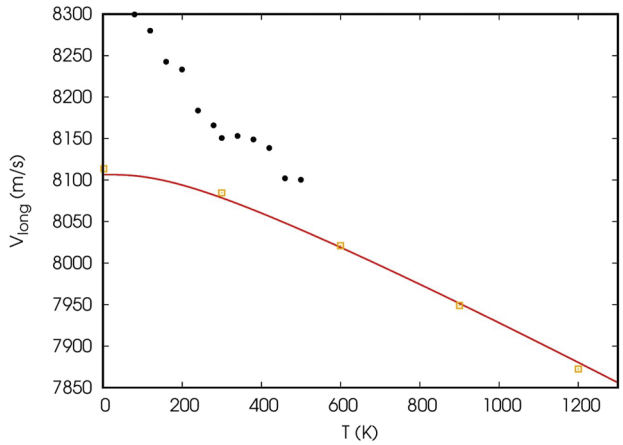

FIG. 3. Longitudinal sound velocity in the 111 direction of BAs computed from TDECs (see Ref. 7) with relaxed-ions at $T = 0$ K (red line) and at finite T (orange points). The experimental data are also reported (black points, extrapolated from Ref. 25).

RI at $T = 0$ K (red line) reported also in Ref. 2 and the new estimate with the ions relaxed at finite temperature (yellow line). The largest effect of the FI approximation is in the zero-temperature EC with a difference of ~300 kbar with respect to the RI case. A non-negligible effect is shown in the temperature dependence of the ECs as well. The red curve is obtained by computing the second derivatives of the free-energy with respect to the strained configurations where the atoms are relaxed at $T = 0$ K: For this reason, the actual correction to the elastic constant depends on temperature. The temperature dependence of the FI estimate (light-blue line) is larger than the other estimates, showing a softening of ~13% in the range of temperatures 0–1200 K, compared to ~8.6% for the relaxed-ions at the $T = 0$ K estimate, and ~4.5% for the finite-temperature relaxed-ion estimate. Hence, there is a visible difference in the TDECs computed with zero-temperature and finite-temperature atomic relaxations. Moreover, this difference increases with temperature.

In Fig. 2, we report the C_{44} EC of BAs, with the colors having the same meaning as in Fig. 1. In the range of temperatures 0–1200 K, the softening of the C_{44} EC is ~10% with frozen-ions, ~8% with the zero-temperature atomic relaxation, and ~7% for the finite-temperature one. Hence, the effect of finite-temperature relaxation is smaller than the one found for Si, but it is still visible and increases with temperature.

With the new C_{44} EC of BAs, we can compute the longitudinal sound velocity in the [111] direction (see Ref. 7 or Ref. 15), compared with the previous calculation and experiment. In Fig. 3, we report the data of Ref. 7 (Fig. 2) with the new velocity (orange points). The differences are very small for the range of temperatures considered.

From the difference between the FI EC curves (blue) and the finite-temperature RI ones (yellow), we obtain the correction $\Delta C_{44}(T)$ at each temperature at the minimum of the free-energy. Then, from Eq. (18), we can write ξ in terms of $\Delta C_{44}(T)$ and, hence,

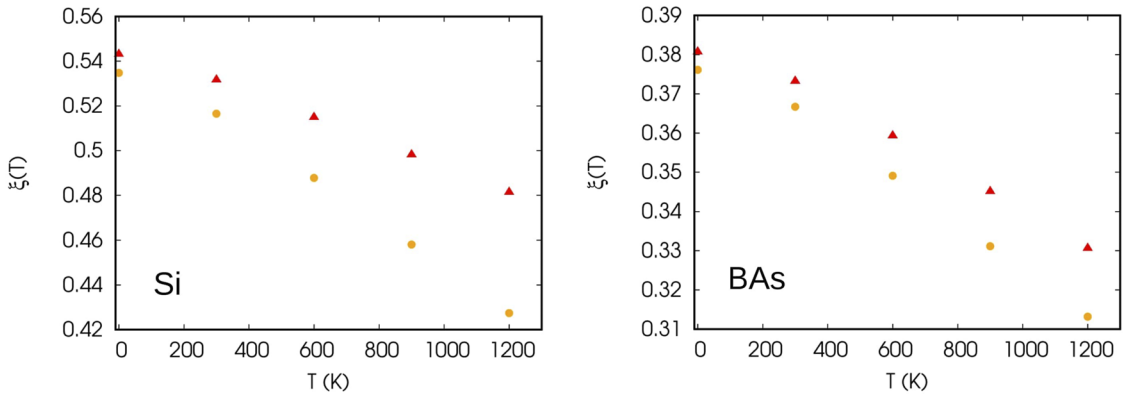

FIG. 4. Temperature-dependent Kleinman parameters for Si (left) and BAs (right) calculated from Eq. (21). The finite-temperature relaxations (yellow circles) are compared with the zero-temperature relaxations (red triangles).

obtain the Kleinman parameter as a function of the temperature $\xi(T)$ as follows:

$$\xi(T) = \frac{2}{\omega_{TO}(T)}\sqrt{\frac{a(T)\Delta C_{44}(T)}{\mu}}, \tag{21}$$

where $a(T) = [4\ \Omega(T)]^{\frac{1}{3}}$ and ω_{TO} is obtained by the interpolation of the frequencies at $\Omega(T)$. The temperature-dependent Kleinman parameters are reported in Fig. 4 (yellow points). They decrease as temperature increases. Hence, in Si, the difference with the experiment $\xi = 0.74(4)$[10] increases as temperature increases as well. We report also $\xi(T)$ obtained by using the correction ΔC_{44} related to the zero-temperature atomic relaxations (the difference between blue and red curves in Figs. 1 and 2). The smaller correction leads to a larger Kleinman parameter and a smaller slope of $\xi(T)$.

V. CONCLUSIONS

We have estimated the effect of atomic relaxation at finite temperature by means of the internal-strain method dealing with the derivatives of the Helmholtz free-energy with respect to both displacements and strain. We showed that internal strain at finite temperature leads to a smaller softening of the C_{44} ECs of Si and BAs with respect to the ZSISA. The temperature induced softening passes from 8.6% (within the ZSISA) to 4.5% (within the temperature-dependent atomic relaxation) in the range 0–1200 K for Si and from 8% (within the ZSISA) to 7% (with the temperature-dependent atomic relaxation) in the same range of temperatures for BAs. Moreover, the differences introduced by the finite-temperature relaxation increase with temperature. We also showed that in our two examples, the Kleinman parameter monotonically decreases with temperature.

ACKNOWLEDGMENTS

Computational facilities were provided by SISSA through its Linux Cluster and ITCS and by CINECA through SISSA-CINECA 2021-2022 agreement.

AUTHOR DECLARATIONS

Conflict of Interest

The authors have no conflicts to disclose.

DATA AVAILABILITY

The data that support the findings of this study are available within the article.

APPENDIX: DISPLACEMENTS OF OPTICAL MODES

The atomic displacement (for atom s, mode ν, and direction α) can be written (at time $t = 0$) as follows:

$$u^{\nu}_{s\alpha} = A^{\nu}\frac{e^{\nu}_{s\alpha}}{\sqrt{M_s}}, \tag{A1}$$

where A^{ν} is the amplitude of the displacement with dimensions $[L]\times[M]^{\frac{1}{2}}$, M_s is the mass of atom s, and $e^{\nu}_{s\alpha}$ is the eigenvector of the displacement. For the optical mode, the eigenvector has the form reported in Eq. (14). If we define the amplitude as

$$A^{\nu} = \sqrt{\mu}u, \tag{A2}$$

where μ is the reduced mass and u is the module of the displacement, we obtain the energy as defined in Ref. 10 as follows:

$$E = \frac{1}{2}\mu\omega^2_{TO}u^2. \tag{A3}$$

With the substitutions of Eqs. (14) and (A2) into Eq. (A1), we obtain the displacements of both atoms as follows:

$$\mathbf{u}^{\nu} = \frac{u}{\sqrt{3}}\begin{pmatrix} \frac{M_2}{M_1+M_2} \\ \frac{M_2}{M_1+M_2} \\ \frac{M_2}{M_1+M_2} \\ -\frac{M_1}{M_1+M_2} \\ -\frac{M_1}{M_1+M_2} \\ -\frac{M_1}{M_1+M_2} \end{pmatrix}. \tag{A4}$$

It is possible to shift the origin of the coordinates in such a way to fix the first atom in the origin. So, we subtract $\frac{u}{\sqrt{3}}\frac{M_2}{M_1+M_2}$ from the components of both atoms, and we have

$$\tilde{\mathbf{u}}^{\nu} = u'\begin{pmatrix} 0 \\ 0 \\ 0 \\ -1 \\ -1 \\ -1 \end{pmatrix}, \tag{A5}$$

where we have also defined $u' = \frac{u}{\sqrt{3}}$. Note that the original displacement (A4) conserves the position of the center of mass $\mathbf{R}_{CM} = \frac{M_1\mathbf{u}_1+M_2\mathbf{u}_2}{M_1+M_2} = 0$, while in the case of the shifted displacements (A5), we have $\mathbf{R}'_{CM} = \frac{-M_2\mathbf{u}_2}{M_1+M_2} \neq 0$. Hence, the internal relaxation of the system of two atoms can be described by keeping the first atom fixed and allowing the second to change its position.

REFERENCES

[1] M. J. Gillan, D. Alfè, J. Brodholt, L. Vočadlo, and G. D. Price, Rep. Prog. Phys. **69**, 2365–2441 (2006).
[2] C. Malica and A. Dal Corso, J. Phys.: Condens. Matter **32**, 315902 (2020).
[3] C. Malica and A. D. Corso, J. Phys.: Condens. Matter **33**, 475901 (2021).
[4] N. L. Allan, T. H. K. Barron, and J. A. O. Bruno, J. Chem. Phys. **105**, 8300 (1996).

[5]L. N. Kantorovich, Phys. Rev. B **51**, 3520 (1995).
[6]L. N. Kantorovich, Phys. Rev. B **51**, 3535 (1995).
[7]C. Malica and A. Dal Corso, J. Appl. Phys. **127**, 245103 (2020).
[8]In principle the sum is extended aver all modes, including the zero-frequency acoustic ones for which Eq. (6) diverges. We do not treat this divergence problem because the acoustic modes will not contribute in the rest of the formulation.
[9]K. Karch, P. Pavone, W. Windl, O. Schütt, and D. Strauch, Phys. Rev. B **50**, 17054 (1994).
[10]O. H. Nielsen and R. M. Martin, Phys. Rev. B **32**, 3792 (1985).
[11]W. R. L. Lambrecht, B. Segall, M. Methfessel, and M. van Schilfgaarde, Phys. Rev. B **44**, 3685 (1991).
[12]P. Giannozzi, S. Baroni, N. Bonini, M. Calandra, R. Car, C. Cavazzoni, D. Ceresoli, G. L. Chiarotti, M. Cococcioni, I. Dabo *et al.*, J. Phys.: Condens. Matter **21**, 395502 (2009).
[13]P. Giannozzi, O. Andreussi, T. Brumme, O. Bunau, M. B. Nardelli, M. Calandra, R. Car, C. Cavazzoni, D. Ceresoli, M. Cococcioni *et al.*, J. Phys.: Condens. Matter **29**, 465901 (2017).
[14]The thermo_pw code can be downloaded from the web page https://dalcorso.github.io/thermo_pw.
[15]C. Malica, Ph.D. thesis, SISSA (International School for Advanced Studies), 2021, https://iris.sissa.it/handle/20.500.11767/125489.
[16]A. Dal Corso, J. Phys.: Condens. Matter **28**, 075401 (2016).
[17]We compute the derivative with respect to the bond length $l = \sqrt{3}u_{21}$, $\frac{\partial E}{\partial l} = \frac{\partial E}{\partial u_{21}}\frac{\partial u_{21}}{\partial l} = \frac{1}{\sqrt{3}}\frac{\partial E}{\partial u_{21}}$: hence, a factor $\sqrt{3}$ is introduced. The other factor, introduced in the derivative with respect to strain, is given by the energy-strain expansion ϵF: $E(\epsilon_F) = E_0 + \sum_{ij}\frac{\partial E}{\partial \epsilon_{ij}}\epsilon_{ij} = E_0 + 6\frac{\partial E}{\partial \epsilon_{23}}\epsilon_{23}$.
[18]J. P. Perdew and A. Zunger, Phys. Rev. B **23**, 5048–5079 (1981).
[19]pslibrary can be dowloaded from the web page https://github.com/dalcorso/pslibrary.
[20]We used pseudopotentials Si.pz-nl-kjpaw_psl.1.0.0.UPF, C.pz-n-kjpaw_psl.1.0.0.UPF, Ga.pz-dnl-kjpaw_psl.1.0.0.UPF, As.pz-n-kjpaw_psl.1.0.0.UPF, and B.pz-n-kjpaw_psl.1.0.0.UPF.
[21]S. Baroni, S. de Gironcoli, A. Dal Corso, and P. Giannozzi, Rev. Mod. Phys. **73**, 515 (2001).
[22]A. Dal Corso, Phys. Rev. B **81**, 075123 (2010).
[23]H. J. McSkimin, J. Appl. Phys. **24**, 988–997 (1953).
[24]C. Malica and A. Dal Corso, Acta Crystallogr., Sect. A: Found. Adv. **75**, 624–632 (2019).
[25]J. S. Kang, M. Li, H. Wu, H. Nguyen, and Y. Hu, Appl. Phys. Lett. **115**, 122103 (2019).